

Transient excitons at metal surfaces

Xuefeng Cui,¹ Cong Wang,¹ Adam Argondizzo,¹ Sean Garrett-Roe,² Branko

Gumhalter,³ and Hrvoje Petek¹

¹Department of Physics and Astronomy, University of Pittsburgh, Pittsburgh PA 15260

²Department of Chemistry, University of Pittsburgh, Pittsburgh PA 15260

³Institute of Physics, HR-10000 Zagreb, Croatia

Abstract

Excitons, electron-hole pairs bound by the Coulomb potential, are fundamental quasiparticles of coherent light-matter interaction energizing processes from photosynthesis to optoelectronics¹⁻⁵. Excitons are observed in semiconductors, and their existence is implicit in the quantum theory of metals, yet their appearance is tenuous due to the screening of the Coulomb interaction on few femtosecond timescale⁶⁻⁸. Here we present direct evidence for the dominant transient excitonic response at a Ag(111) surface, which precedes the full screening of the Coulomb interaction, in the course of a three-photon photoemission process with <15 femtosecond laser pulses. Electron-hole pair interaction through the excitonic response introduces coherent quasiparticle correlations beyond the single-particle description of the optics of metals, which dominate the multi-photon photoemission process.

Reflection of light has made metal mirrors valued optical instruments since the bronze age⁹. At the macroscopic level the coherent optical response of a metallic surface is well described by the classical Maxwell's equations. At the quantum level, a photon interacting with a metal surface polarizes an electron-hole (e - h) pair to create an exciton-polariton, the quasiparticle of light-matter interaction¹⁰. The creation of excitons in insulators, semiconductors, and molecules provokes many-body, coherent optical processes, which have been studied in contexts of photosynthesis, vision, optical communication¹⁻⁵, etc. Yet in metals, the role of excitons remains uncharted, because screening building up on the timescale of plasma oscillation liberates bound states of the Coulomb potential⁶⁻⁸. The dynamical response of a metal surface to light terminates either in reflection, which is coherent, or absorption, which can be detected through the photoelectric effect¹¹.

We reveal the transient optical response of the Ag(111) surface triggered by electron from the Shockley surface state (SS) absorbing a photon to form instantaneously the primary exciton. In response, the screening charge density fluctuations cause the bare Coulomb potential binding the exciton to wane, and simultaneously the image potential (IP) binding the electron to its screening image charge, to emerge as the asymptotic state of the quasiparticle interacting with its medium. This transient regime of the coherent excitonic polarization is revealed by a new mode of surface photoemission via m^{th} -order multiphoton absorption.

Coherent optical response of metals has been studied by energy (E) and momentum (k) resolved multiphoton photoemission ($m\text{PP}$) spectroscopy. Interferometric time-resolved 2PP measurements¹² determined surface and bulk

electron and hole dephasing on femtosecond timescales¹³⁻¹⁵. 2PP studies on silver have probed the dephasing and lifetimes of intermediate IP states¹⁶⁻¹⁸. Attosecond studies have revealed band-dependent photoelectron emission delays¹⁹. In every case, light was thought to excite transitions between preexisting electronic bands.

Excitons in metals have been more illusive. The excitonic response has been discussed in the context of theoretical modeling of the dielectric functions of metals²⁰⁻²². The transient excitonic response, however, has been proposed to have potentially observable consequences in ultrafast *m*PP spectroscopy^{23,24}.

Here we reveal the excitonic response in *m*PP spectra of the Ag(111) surface upon excitation near the two-photon IP \leftarrow SS transition (Fig. 1) by intense, broadly tunable laser pulses with <15 fs duration. For non-resonant excitation, the SS and IP state energy-momentum distributions [$E(k)$; Figs. 2a, h] appear as dispersive bands such as reported in 2PP studies employing two-colour incoherent excitation¹⁸. A dramatic change in *m*PP spectra arises when the laser spectrum overlaps with the two-photon IP \leftarrow SS transition at $\hbar\omega_{res}=1.93\pm0.02$ eV. A new feature that dominates the 3PP spectra (Figs. 2b-g), but does not exist in the single-particle band structure (Fig. 1a), appears at the final state energy $E_f=5.82\pm0.03$ eV above the Fermi level (E_F). Because of its nondispersive character, more than 100 times higher intensity than the non-resonantly excited SS and IP bands (Figs. 2a, h), and photon energy independent photoemission energy, we attribute it to the transient exciton (TE).

Plotting E_f for the SS, IP, and TE features against the excitation photon energy, $\hbar\omega_{laser}$, we find linear behaviour with approximate slopes of three, one, and zero (Fig. 3). This would be expected within Einstein's model of the photoelectric

effect¹¹, where the single-particle energy level and $\hbar\omega_{laser}$ define the photoelectron energy, if SS, IP, and TE were the initial, penultimate, and final states in a 3PP process. Because a discrete state at $E_f=5.82$ eV that could explain TE does not exist (Fig. 1a)²⁵, we will argue that TE manifests a correlated mode of non-Einsteinian photoemission.

Gumhalter *et al.* elaborated an excitonic model for 2PP from the occupied Shockley surface states of Ag(111) or Cu(111) surfaces via the intermediate IP states, which approximately describes our experiment²⁴. Whereas the SSs are Bloch states derived by the surface boundary conditions, the IP states emerge through the many-body screening response²⁶. Excitation of SS within the Drude free-electron continuum can only create the primary exciton state²⁴, because there is no transition moment to the unformed IP state. In response to excitation, charge density fluctuations screen the Coulomb field and thereby produce the screened electron and hole quasiparticles. Upon saturation of the screening, the IP state emerges as on-the-energy-shell, asymptotically evolved excited surface electron state²⁴. The saturation, however, is metal dependent: in silver it takes ~ 15 fs because of its sharp and low frequency (3.7 eV) surface plasmon, whereas for copper it is complete within ~ 2 fs²⁴.

The surface exciton on Ag(111) is composed of the SS hole interacting with the upper *sp*-band (*Usp*) electron Bloch states (Fig. 1a)^{24,27}. Wavefunction of the exciton described by N , the quantum number for relative motion, and \mathbf{K} the total center-of-mass momentum wavevector, may be written as a superposition (wavepacket) of the coupled hole \mathbf{k}_h and electron \mathbf{k}_e momentum states²⁷,

$$|\mathbf{K}, N\rangle = \sum_{\mathbf{k}_e, \mathbf{k}_h} \Psi_{\mathbf{k}_e, \mathbf{k}_h}^{\mathbf{K}, N} |\mathbf{k}_e, \mathbf{k}_h\rangle, \quad (1)$$

where $\Psi_{\mathbf{k}_e, \mathbf{k}_h}^{\mathbf{K}, N}$ is the amplitude of the constituent band states contributing to the exciton in the k -space, and $\mathbf{K} \approx 0$ is imparted by the photon²⁷. The excitonic eigenenergies (Fig. 1b) are obtained by solving the Schrödinger equation for the bare Coulomb potential of the SS-hole charge density²⁴.

The salient features of an exciton expressed in Equation (1) directly explain two facets of the TE behaviour: *i*) the nondispersive TE photoemission derives from it being a localized superposition state in the relative coordinate space constrained by $\mathbf{K} = \mathbf{k}_e + \mathbf{k}_h \approx 0$; and *ii*) its optical transition moment enhancement derives from the summation over the available interband transitions. The congruence of the $k_{||}$ ranges of TE and SS attests to TE being the superposition of all SS states within its 63 meV occupied bandwidth.

To illuminate the role of TE as a precursor to IP in a two-photon $\text{IP} \leftarrow \text{SS}$ transition, we image the photoelectron $E(k)$ distributions as a function of delay τ between identical, collinear, phase-correlated pump-probe pulses. Acquiring $E(k)$ distributions in delay intervals of $\tau \sim 100$ attoseconds for $\hbar\omega_{\text{laser}} = 2.05$ eV records a movie of the TE dynamics (Supplementary Movie S1). The interferogram for $k_{||} = 0 \text{ \AA}^{-1}$ and $E(k)$ distribution for $\tau = 0$ fs (Fig. 4a and b) are cross-sections through the three-dimensional (E, k, τ) data. Correlation traces (Fig. 4c-e) representing cross-sections through the interferogram for E_f marked by the lines cutting Fig. 4a reveal the $E(k)$ -resolved coherent polarization dynamics of SS, IP, and TE.

Instead of single-point correlations, we analyze the co-relationship between the SS, IP, and TE polarizations by Fourier transforming the interferograms for three representative values of $k_{||}$ to obtain 2D spectra of the linear polarization vs. photoelectron energy relative to the SS band minimum (Figs. 4f-h; Supplementary Fig. S1 gives the complete 2D spectra including the weak nonlinear components). We note that even for a detuning $\Delta = \hbar\omega_{laser} - \hbar\omega_{res} = 0.12$ eV the TE response at the polarization energy $\hbar\omega_{res}$ dominates the 2D spectra above the IP state at $\hbar\omega_{laser}$ (Figs. 4f, g). This indicates that the internal field at the IP \leftarrow SS two-photon resonance drives the surface response more effectively than the external laser field. Furthermore, the disposition of the dominant TE and weaker SS responses along the line with the slope of 1/3 (Figs. 4f, g) signifies their origin in coherent 3PP processes of primary states driven by the linear polarization fields.

Being retarded the IP state cannot participate in a coherent 3PP process, and therefore its disposition within the 2D spectra is distinct from those of TE and SS (Figs. 4f-h). Because the IP state appearance does not correlate with the occupied $k_{||}$ range of SS (Fig. 4h), and its alignment is with the slope of 1/2, we conclude that it is excited from the lower sp -band (L_{sp} : Fig. 1a) by absorption of two photons at $\hbar\omega_{laser}$ from the external field. The weak dependence of the IP state with $k_{||}$ indicates that for $\Delta=0.12$ eV, the L_{sp} channel dominates the 3PP via the IP state, even when the TE channel is available. The emergence of the IP state from the TE channel and its subsequent photoemission by a single photon process, however, can be discerned in the additional density in 2D spectra for $|k_{||}| < 0.07 \text{ \AA}^{-1}$, which extends between TE and IP features along the line with a slope of 1 (Figs. 4f, g). The presence of two channels

for IP state photoemission via interactions with the $\hbar\omega_{res}$ and $\hbar\omega_{laser}$ fields leads to the polarization beating in its correlation trace at $\tau \cong 20$ fs (Fig. 4d). A frequency analysis of the interferogram in Fig. 4a shows that the IP state photoemission driven by $\hbar\omega_{laser}$ dominates for <20 fs to be overtaken by the more slowly dephasing TE channel at $\hbar\omega_{res}$. As $\Delta \rightarrow 0$, model simulations of two-pulse correlations (Supplementary Fig. S2) together with 3PP measurements (Fig. 2) support the scenario for the dominant IP state creation from the excitonic manifold.

The 2D spectra explain the final characteristic of the excitonic photoemission, namely the $\hbar\omega_{laser}$ independent TE photoemission energy. Upon femtosecond pulse illumination, an electron is excited by two-photon interaction from SS through a manifold of excitonic states converging in a quasicontinuum to the bottom of U_{sp} (Fig. 1b). Concurrently, the screening response involving off-the-energy-shell transients dominated by the virtual surface plasmon excitation and constrained by the Heisenberg energy-time uncertainty evolves the bare exciton into its saturated form, the $n=1$ IP electron and the corresponding SS hole quasiparticle pair²⁸. In the course of this quantum kinetic evolution the virtual excitations die off through destructive interference and only the energy conserving excitations persist. Therefore, a local field can grow only at $\hbar\omega_{res}$ associated with the coherent coupling of the entire SS-band to form the asymptotic IP state. Because TE photoelectrons emerge by multiple quantum absorption from the excitonically enhanced local field at $\hbar\omega_{res}$, the TE energy does not track $\hbar\omega_{laser}$ ^{29,30}.

The correlated TE photoemission and its associated local field are manifestations of the fundamental screening response of solid-state matter to

polarization by external optical fields. Although excitons are detected as stable quasiparticles in semiconductors and insulators, the dynamical dielectric response involved in their formation and propagation is universal, and should be observable in other materials. For example, the new mode of local field-induced photoemission driven by multiple-quantum transient exciton interactions in silver may illuminate the multi-exciton generation in organic films¹. The inducing and probing of strong e - h correlations even in a noble metal silver by coherent multiphoton photoemission spectroscopy, holds promise for extending to nonequilibrium quasiparticle dynamics in more strongly correlated materials.

Methods summary

Femtosecond laser excitation. The photoexcitation source for the *mPP* measurements is a noncollinear parameter amplifier (NOPA) system pumped by Clark MXR Impulse fiber-laser oscillator-amplifier system. The NOPA system is used >100 mW average power at 1.25 MHz repetition rate with <15 fs pulse duration. The p-polarized light incident at 45 ° from the surface normal is focused onto ~100 μm diameter spot at the Ag(111) sample.

Interferometric pump-probe delay scanning. Identical pump-probe pulse replicas are generated in a self-made Mach-Zehnder Interferometer (MZI)^{12,13}. The pump-probe delay is scanned with a piezoelectrically actuated translation stage at a rate of 7.9 fs/s. Recording interference fringes at the center laser wavelength by passing the secondary output of the MZI through a monochromator, and recording the resulting interferogram with a photodiode calibrates the delay scanning. After

data acquisition, the about 200 interferometric scans are combined in software using the calibration interference fringes.

Photoelectron imaging. The *mPP* photoelectron images are recorded with a Specs Phoibos 100 electron spectrometer equipped with a 3D-DLD delay-line photoelectron counting detector. For each interferometer pump-probe delay scan, 4096 $E(k)$ images are taken with an integration time of 12ms/image.

Sample. The single crystal Ag(111) surface is prepared by conventional surface science methods in an ultrahigh vacuum chamber with a base pressure of $<10^{-10}$ mbar. During the measurements the sample is cooled to ~ 100 K.

Figures

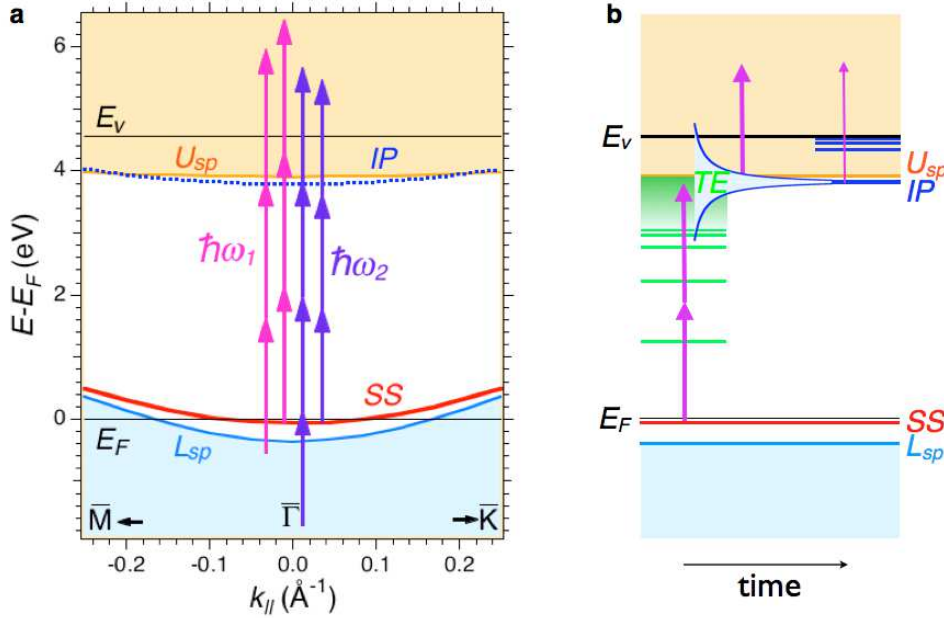


Figure 1

Figure 1. The electronic band structure and multiphoton photoemission processes at Ag(111) surface. **a**, The surface projected band structure of Ag(111) has a band gap extending between -0.4 and 3.9 eV from the lower to the upper sp -band (L_{sp} and U_{sp}). Within the band gap, the Shockley surface state, SS (red line) and $n=1$ IP state (blue dotted line) with minima at -0.063 and 3.79 eV form quantum wells at the metal-vacuum interface. SS is occupied to $|k_{||}|=0.07 \text{ \AA}^{-1}$ where it intersects the Fermi level (E_F). The $n=1$ IP state is the first member of a Rydberg-like series converging to the vacuum level, E_v ^{18,26}. The vertical arrows indicate independent excitation pathways for 3PP and 4PP via the initial SS or the

penultimate IP states for $\hbar\omega_1=2.20$ and $\hbar\omega_2=1.81$ eV. **b**, The excitation scheme of IP states via the transient exciton, TE, manifold. The eigenstates of the excitonic manifold are obtained by solving the Schrödinger equation for bare Coulomb potential of the SS hole (green lines); they converge in a quasi-continuum (shaded green) to the bottom of U_{sp} ²⁴. Charge density fluctuations screening the Coulomb field evolve the bare exciton into the fully screened IP state. The coherent 3PP measurements follow the time evolution of the polarization amplitude within the excitonic manifold towards the asymptotic IP state under the influence of time-dependent potentials and energy-time uncertainty, which is implied by the time-evolving width of the IP state.

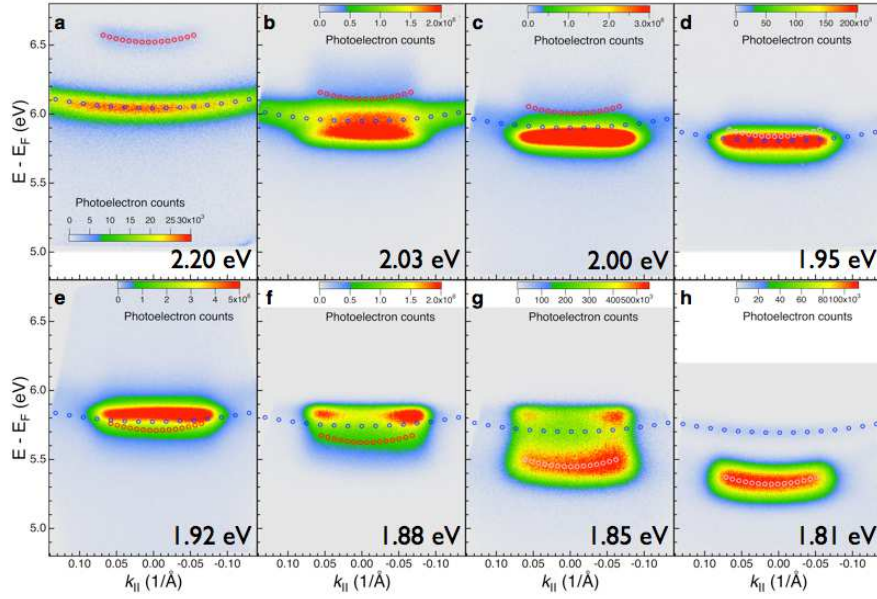


Figure 2

Figure 2. 3PP and 4PP $E(k)$ distributions for photon excitation energies near the two-photon $\text{IP} \leftarrow \text{SS}$ resonance. **a** and **h**, For nonresonant excitation at $\hbar\omega_{\text{laser}} = 1.81$ and 2.20 eV the SS and IP bands appear with $E(k)$ dispersions consistent with the band structure and excitation processes indicated in Fig. 1a; the red and blue circles denote their expected parabolic dispersions. **b – g**, Upon tuning $\hbar\omega_{\text{laser}}$ into the two-photon $\text{IP} \leftarrow \text{SS}$ resonance, a new feature characterized by enhancement of the transition moment, non-dispersive, i.e. flat, $E(k)$ distribution spanning the occupied $k_{||}$ range of SS, and photon energy independent photoelectron energy appears at $E_f = 5.82 \pm 0.03$ eV. We attribute these characteristics to a transient excitonic state created by excitation of an electron from SS via the excitonic manifold, through a two-photon resonance involving the energy conserving IP state. The photoelectron energies are given with respect to E_F .

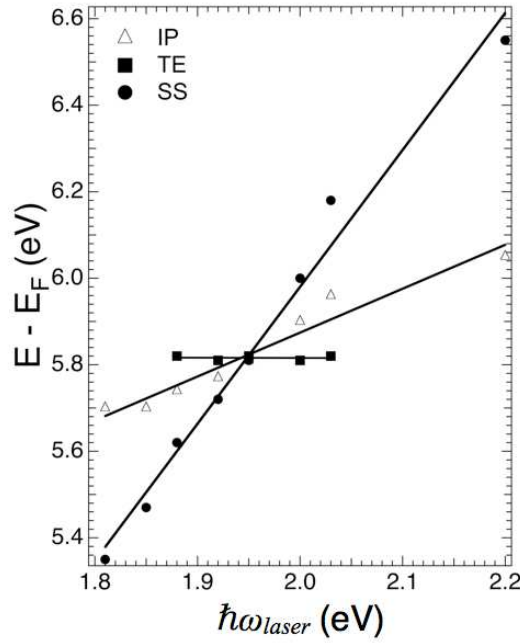


Figure 3

Figure 3. The tuning of the spectroscopic features with photon energy. The photoelectron energies of SS, IP, and TE states in Fig. 2 are plotted vs. the excitation photon energy. According to Einstein's model, the photoelectron energy in a photoemission process is defined by the photon energy. In a multiphoton process, the tuning of the photoelectron energy E_f of a spectroscopic feature is determined by the number of photons times the photon energy required to excite an electron from it to above E_v . Therefore, in the 3PP process, the initial state (SS) is expected to tune with a slope of three and the penultimate state (IP) with a slope of one, as observed. Accordingly, the slope of zero would attribute the TE feature to a sharply defined state at $E_f=5.82\pm0.03\text{eV}$, which does not exist in the band structure of Ag. The TE behavior therefore implies a previously unknown, non-Einsteinian photoemission process where resonantly enhanced local field associated with the excitonic polarization of the sample excites the TE photoemission.

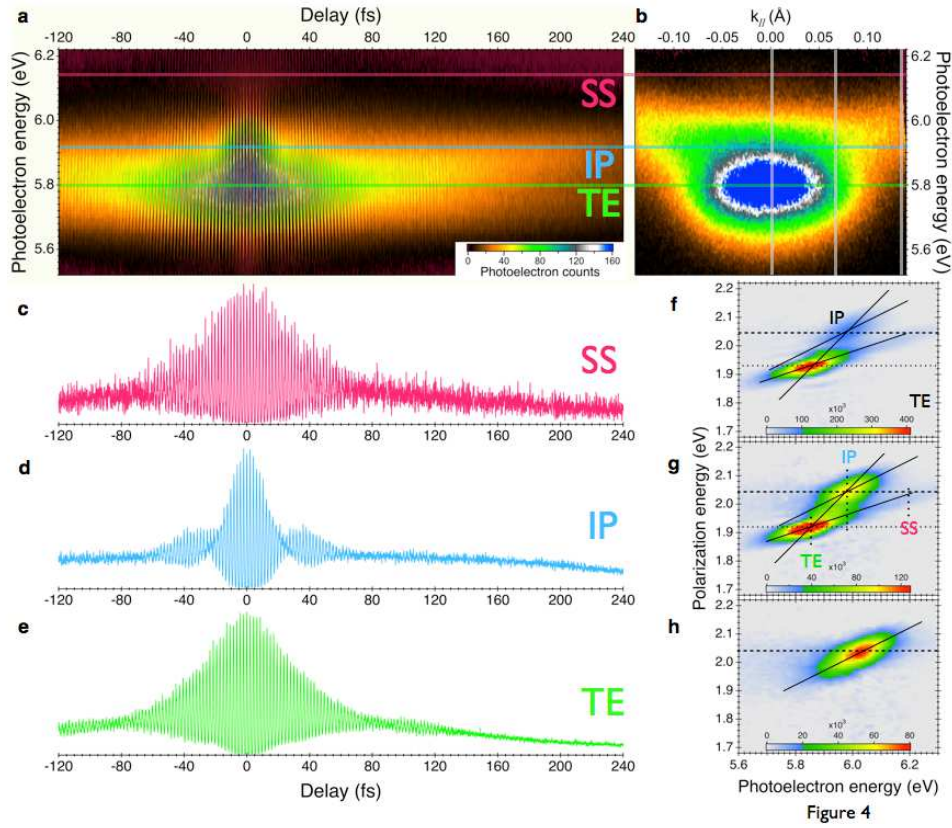


Figure 4. 3D photoemission spectra for near-resonant two-photon IP \leftarrow SS excitation. **a**, The interferogram of photoelectron counts vs. photoelectron energy and time delay between interferometrically scanned pump-probe pulses for $k_{||}=0$. The $\hbar\omega_{laser}=2.05$ eV is detuned from the resonance energy, $\hbar\omega_{res}=1.93$ eV. **b**, The $E(k)$ image at zero pump-probe delay. The horizontal lines indicate the energies of the SS, IP, and TE signals, and the vertical lines indicate momenta for the 2D spectra in **f-h**. **c-e** Correlation measurements¹³ obtained by taking cross sections through the interferogram in **a** at the energies of SS, IP, and TE. The oscillations with approximately the period of the carrier wave (~ 2 fs) represent the interference between the pump and probe pulse-induced polarizations excited in the sample. **f-h**, 2D photoelectron spectra obtained by Fourier transforming the interferometric

scans such as in **a** for $k_{||}=0.0$ (**f**), 0.067 (**g**), and 0.134 \AA^{-1} (**h**). The Fourier axis is labeled the “polarization energy”. Higher order polarization components are substantially weaker (Supplementary Fig. S1). The 2D plots show the correlation between the coherent polarization and photoemission energy. The dashed and dotted lines indicate $\hbar\omega_{laser}$ and $\hbar\omega_{res}$, the vertical lines indicate the energies of the SS, IP, and TE signals, and the full lines designate the slopes of $\frac{1}{3}$, $\frac{1}{2}$, and 1 .

References

- 1 Chan, W.-L. *et al.* Observing the Multiexciton State in Singlet Fission and Ensuing Ultrafast Multielectron Transfer. *Science* **334**, 1541-1545 (2011).
- 2 Gibbs, H.M., Khitrova, G., & Koch, S.W. Exciton-polariton light-semiconductor coupling effects. *Nat Photon* **5**, 273-273 (2011).
- 3 Turner, D.B. & Nelson, K.A. Coherent measurements of high-order electronic correlations in quantum wells. *Nature* **466**, 1089-1092 (2010).
- 4 Cundiff, S.T. & Mukamel, S. Optical multidimensional coherent spectroscopy. *Physics Today* **66**, 44-49 (2013).
- 5 Lee, H., Cheng, Y.-C., & Fleming, G.R. Coherence Dynamics in Photosynthesis: Protein Protection of Excitonic Coherence. *Science* **316**, 1462-1465 (2007).
- 6 Edwards, P.P., Lodge, M.T.J., Hensel, F., & Redmer, R. '... a metal conducts and a non-metal doesn't'. *Phil. Trans. R. Soc. A* **368**, 941-965 (2010).
- 7 Silkin, V.M., Kazansky, A.K., Chulkov, E.V., & Echenique, P.M. Time-dependent screening of a point charge at a metal surface. *J. Physics: Condens. Matter* **22**, 304013 (2010).
- 8 Huber, R. *et al.* How many-particle interactions develop after ultrafast excitation of an electron-hole plasma. *Nature* **414**, 286-289 (2001).
- 9 Enoch, J.M. History of Mirrors Dating Back 8000 Years. *Optometry & Vision Science* **83**, 775-781 (2006).
- 10 Hopfield, J.J. Theory of the Contribution of Excitons to the Complex Dielectric Constant of Crystals. *Phys. Rev.* **112**, 1555 (1958).
- 11 Einstein, A. Über einen die Erzeugung und Umwandlung des Lichtes betreffenden heuristischen Standpunkt. *Annalen der Physik* **17**, 132 (1905).
- 12 Petek, H. & Ogawa, S. Femtosecond Time-Resolved Two-Photon Photoemission Studies of Electron Dynamics in Metals. *Prog. Surf. Sci.* **56**, 239-310 (1997).
- 13 Ogawa, S., Nagano, H., Petek, H., & Heberle, A.P. Optical dephasing in Cu(111) measured by interferometric two-photon time-resolved photoemission. *Phys. Rev. Lett.* **78**, 1339-1342 (1997).
- 14 Petek, H., Nagano, H., & Ogawa, S. Hole Decoherence of d Bands in Copper. *Phys. Rev. Lett.* **83**, 832-835 (1999).
- 15 Gütde, J. *et al.* Time-Resolved Investigation of Coherently Controlled Electric Currents at a Metal Surface. *Science* **318**, 1287-1291 (2007).
- 16 Giesen, K. *et al.* Image Potential States Seen via Two-Photon Photoemission and Second Harmonic Generation. *Physica Scripta* **35**, 578 (1987).
- 17 Schoenlein, R.W., Fujimoto, J.G., Eesley, G.L., & Capehart, T.W. Femtosecond relaxation dynamics of image-potential states. *Phys. Rev. B* **43**, 4688-4698 (1991).
- 18 Marks, M. *et al.* Quantum-beat spectroscopy of image-potential resonances. *Phys. Rev. B* **84**, 245402 (2011).
- 19 Cavalieri, A.L. *et al.* Attosecond spectroscopy in condensed matter. *Nature* **449**, 1029-1032 (2007).
- 20 Mueller, F.M. & Phillips, J.C. Electronic Spectrum of Crystalline Copper. *Phys. Rev.* **157**, 600 (1967).

- 21 Fong, C.Y. *et al.* Wavelength Modulation Spectrum of Copper. *Phys. Rev. Lett.* **25**, 1486 (1970).
- 22 Marini, A. & Del Sole, R. Dynamical Excitonic Effects in Metals and Semiconductors. *Phys. Rev. Lett.* **91**, 176402 (2003).
- 23 Schöne, W.-D. & Ekardt, W. Transient excitonic states in noble metals and Al. *Phys. Rev. B* **65**, 113112 (2002).
- 24 Gumhalter, B., Lazić, P., & Došlić, N. Excitonic precursor states in ultrafast pump-probe spectroscopies of surface bands. *phys. stat. sol. (b)* **247**, 1907-1919 (2010).
- 25 Miller, T., Hansen, E.D., McMahon, W.E., & Chiang, T.C. Direct transitions, indirect transitions, and surface photoemission in the prototypical system Ag(111). *Surf. Sci.* **376**, 32-42 (1997).
- 26 Echenique, P.M. & Pendry, J.B. Theory of image states at metal surfaces. *Prog. Surf. Sci.* **32**, 111 (1990).
- 27 Elliott, R.J. Intensity of Optical Absorption by Excitons. *Phys. Rev.* **108**, 1384-1389 (1957).
- 28 Gumhalter, B. Stages of hot electron dynamics in multiexcitation processes at surfaces: General properties and benchmark examples. *Prog. Surf. Sci.* **87**, 163-188 (2012).
- 29 Merschdorf, M., Kennerknecht, C., & Pfeiffer, W. Collective and single-particle dynamics in time-resolved two-photon photoemission. *Phys. Rev. B* **70**, 193401 (2004).
- 30 Winkelmann, A. *et al.* Resonant coherent three-photon photoemission from Cu(001). *Phys. Rev. B* **80**, 155128-155129 (2009).

Acknowledgements

This research was supported by Division of Chemical Sciences, Geosciences, and Biosciences, Office of Basic Energy Sciences of the U.S. Department of Energy through Grant DE-FG02-09ER16056.

Author contributions

H.P. conceived the experiment and wrote the first draft of the manuscript. X.C. and C.W. discovered the transient exciton in Ag(111), set up the photoelectron imaging system, wrote the data acquisition and analysis programs, and performed all of the experiments and data analysis. A.A. set up the NOPA system and contributed to its operation. S.G.R. provided the expertise in 2D electronic spectroscopy. B.G. predicted the TE phenomenon and performed the theoretical simulations. All coauthors contributed to the discussion and elucidation of the TE phenomenon.

Additional Information

Supplementary information is available in the online version of the paper on www.nature.com/naturephysics. Reprints and permissions information is available online at www.nature.com/reprints. Correspondence and requests for materials should be addressed to H.P. .

Competing Financial interests

The authors declare no competing financial interests.